Radar Systems for Infrastructures Diagnostics: A Review

Ilaria Catapano, Antonio Affinito, Lorenzo Crocco, Francesco And Soldovieri

RADAR SYSTEMS FOR INFRASTRUCTURES DIAGNOSTICS: A REVIEW

Ilaria Catapano, Antonio Affinito, Lorenzo Crocco, Francesco Soldovieri

IREA, CNR, via Diocleziano 328, I-80124, Napoli, ITaly

soldovieri.f@irea.cnr.it

ABSTRACT

This communication aims at summarizing the main features, recent advancements and examples assessing the reconstruction capabilities of two different radar systems for subsurface imaging and civil engineering monitoring and diagnostics. In fact, Ground Penetrating Radar and Holographic Radar are well assessed non-invasive tools capable of investigating the inner status of an object and are attracting more and more attention in several applicative scenarios, for their easiness of use and significant imaging capabilities.

KEYWORDS: *Ground Penetrating Radar, Holographic Radar, Microwave Imaging, Subsurface imaging.*

INTRODUCTION

Non-invasive and safety diagnostic tools capable of providing information about objects' inner are hugely demanded in a large number of applicative scenarios, among which structural diagnostics and monitoring. In this specific applicative framework, the main goal is to make it available systems capable of providing reliable and high resolution images of the observed region, from which it is possible to acquire information on the architectural features of buildings and infrastructures as well as on the risk factors affecting their integrity, such as deformations and oxidization of the reinforcement bars, water infiltrations, crack and air gaps. The availability of such an information is, indeed, crucial not only to properly plan and timely address maintenance actions but also to assess the effectiveness of restoration works.

Such a requirement motivates on one hand the design and the performance evaluation of novel technologies and systems and on the other side the development of advanced data processing methodologies aimed at enhancing the imaging capabilities of the overall survey/diagnostics procedure.

Among the non invasive diagnostic techniques currently at the state of art, radar systems are worth to be considered. As a matter of fact, they are able to attain high resolution images of the hidden features of a surveyed spatial region by exploiting the ability of the microwaves to penetrate inside opaque materials. However, despite the simple electromagnetic sensing mechanism , their use in operative conditions is not with immediate impact. This is mainly due to the fact that the provided raw radar images suffer of "blurring" effects, which make their interpretation very difficult and prone to the operators' expertise. Therefore, a continuous research effort is on-going so to address the development of novel hardware solutions and of data processing strategies, with the final aim of providing easily interpretable images, possibly in real-time.

In this frame, this communication aims at summarizing the main features in terms of imaging capabilities of two different kind of subsurface radar systems, available at the Institute for Electromagnetic Sensing of the Environment - National Research Council of Italy (IREA-CNR).

First of all, Ground Penetrating Radar (GPR) systems enhanced by an advanced data processing approach, commonly known as Microwave Tomography [1], are presented. GPR systems are well known tools for non-invasive in situ surveys and Microwave Tomography (MWT)

refers to a model based data processing approach, which recasts the imaging as a linear inverse scattering problem [1]. Such an approach has been already tested in a large number of real test sites and it is capable of providing stable and high resolution images, which allows us to infer the geometrical features of hidden targets [2-6]. These images are obtained by computationally efficient approaches able to comply with the real world situations.

The second system available at IREA is a holographic systems [7,8], designed by Remote Sensing Laboratory of Bauman Moscow State Technical University. This system records the amplitude of the interference signal arising between the backscattered field and a reference signal. Therefore, provided that a constructive interference arises, it provides high resolution images of hidden targets in real-time and without involving nay sophisticated data processing. At the present, the main drawback is that information on targets depth is totally missed.

The present communication is organized as it follows. In Section 1 a brief description of the main features of MWT enhanced GPR systems is given while Section 2 deals with a test case exemplifying the achievable performance in the frame of structural monitoring. After, the holographic system Rascan 4/4000 and its working principle are summarized in Section 3; imaging capabilities of the holographic radar are presented in Section 4 thanks to experiments carried out in laboratory controlled conditions. Conclusions follow.

1 MICROWAVE TOMOGRAPHY ENHANCED GPR

GPR is a well assessed technology and several commercial systems have been developed and widely adopted in many applicative conditions [9]. The working principle is the same as a traditional radar, i.e., a transmitting antenna radiates a probing wave into the investigated medium (a soil, a wall, a road and so on) and a single (standard GPR) or multiple (array GPR) receiving antennas are used to collect the field backscattered by the targets.. GPR is usually designed to work in time domain but radar working also in frequency domain are commercially available. IREA has the availability of the time-domain radar depicted in Fig.1. The radar is equipped with a dual frequency single fold shielded antenna system working at the nominal central frequencies of 200 MHz and 600 MHz for subsurface prospecting and a single frequency and single fold shielded antennas with nominal central frequency of 2 GHz for vertical inspections.

Figure 1: GPR system available at IREA-CNR equipped with the dual frequency antenna system working at the nominal central frequencies of 200 MHz and 600 MHz.

Generally speaking, an time-domain GPR system transmits a modulated time domain pulse and collects the reflected energy as a function of time, which represents the travel-time of the wave along the transmitter-target-receiver path. By shifting the transmitting and receiving antennas along a line and joining together the gathered traces at all the antenna positions, a spatial-time image is built, which is referred to as raw-data “radargram” or B-scan. Being the round-trip travel time a

function of the distance occurring between antennas and targets, the radargram provides a distorted image of the hidden objects, which appear as hyperbolas whose characteristic features (i.e., vertex and eccentricity) depend on the object position, shape, size and electromagnetic properties of the probed medium. By processing the radargram, it is in principle possible to obtain images providing a complete characterization in terms of geometrical parameters (i.e., location, size and shape) and electromagnetic features (i.e., relative permittivity and dielectric conductivity) of hidden objects and/or material changes. Of course, this involves the use of sophisticated data processing approaches based on an accurate model of the electromagnetic scattering and capable of solving accurately the relevant non-linear inverse scattering problem [10].

Among the data processing strategies proposed in the GPR literature, a significant role is played by the MWT [1]. In particular, we referee to an imaging approach based on an integral frequency domain integral formulation based on Born Approximation to describe the relationship between the scattered field (i.e. the data) and the electric unknown contrast function. This contrast function accounts for the target as an anomaly in terms of electromagnetic properties with respect to the ones of the of the background medium. The imaging is faced as the solution of a linear inverse scattering problem and a stable solution is obtained by using the Truncated Singular Value Decomposition (TSVD) [10].

In details, let $E_s(\mathbf{r}_m, \mathbf{r}_s, \omega)$ be the scattered field measured at the generic point $\mathbf{r}_m$ and angular frequency ω when the transmitting antenna is in $\mathbf{r}_s$ and $\chi(\mathbf{r}) = (\varepsilon_x(\mathbf{r})/\varepsilon_b - 1)$ the unknown electric contrast function, $\varepsilon_x(\mathbf{r})$ being the unknown (complex) permittivity and ε_b that of the probed medium, $\mathbf{r}_m$, $\mathbf{r}_s$ are on the measurement surface Γ and $\mathbf{r}$ is a generic point into the investigated domain Ω The scattering is described by the linear integral equation:

$$E_s(\mathbf{r}_m, \mathbf{r}_s, \omega) = k_b^2 \int_D G(\mathbf{r}_m, \mathbf{r}, \omega) E_{inc}(\mathbf{r}, \mathbf{r}_s, \omega) \chi(\mathbf{r}) d\mathbf{r} \tag{1}$$

After the discretization of the integral equation (1), the imaging is faced by solving the matrix inversion problem:

$$\mathbf{E}_s = \mathbf{L}\boldsymbol{\chi} \tag{2}$$

where $\mathbf{E}_s$ is the K=M x F dimensional data vector, M being the number of spatial measurement points and F the number of working frequencies, $\boldsymbol{\chi}$ is the N dimensional unknown vector, N being the number of points in Ω, and $\mathbf{L}$ is the K x N dimensional matrix obtained by discretizing the integral operator in eq.(1). The matrix inversion problem stated by eq.(2) is ill-conditioned and a regularized solution with respect to measurement uncertainties and noise is given by:

$$\tilde{\chi}(\mathbf{r}) = \sum_{n=1}^{T} \frac{\langle \mathbf{E}_s, \mathbf{u}_n \rangle}{\sigma_n} \underline{v}_n(\mathbf{r}) \tag{3}$$

In eq.(3), $\langle \cdot, \cdot \rangle$ denotes the scalar product in the data space, T is the truncation threshold, $\{\sigma_n\}_{n=1}^{K}$ is the set of singular values of the matrix $\mathbf{L}$ ordered in a decreasing way, $\{\mathbf{u}_n\}_{n=1}^{K}$ and $\{\mathbf{v}_n\}_{n=1}^{K}$ are the sets of the singular vectors. The threshold $T \leq K$ defines the "degree of regularization" of the solution and is chosen as a trade-off between accuracy and resolution requirement from one side (which should push to increase the T value) and solution stability from the other side (which should push to limit the value of the threshold T).

The imaging result is given as the spatial map of the modulus of the retrieved contrast vector $\tilde{\chi}$ normalized to its maximum value. Hence, the regions of Ωwhere the modulus of $\tilde{\chi}$ is significantly different from zero provide indication on the position and geometry of the targets.

2 MWT enhanced GPR AS A TOOL FOR STRUCTURAL MONITORING

In the last ten years MWT enhanced GPR surveys have been carried out in several test cases concerning with applicative fields ranging from archeology to environmental surveys [2-6].

As an example of the achievable performances in the specific field of structural monitoring, we show the results concerning an experiment carried out in the framework of the FP7-research project 'Integrated System for Transport Infrastructure Surveillance" [11] at the Montagnole test site, a facility of the French Institute of Science and Technology for Transport, Development and Networks. The test site and the experiment are fully described in [6], wherein a detailed discussion on the reconstruction capabilities offered by MWT enhanced GPR is also provided.

The experiment aimed at assessing the ability to detect inner damages of a reinforced concrete beam subjected to strong mechanical solicitations reproducing the occurrence of critical events. In particular, a 16 m long, 0.5 m width and 1 m high beam has been affected by direct impacts of a 2500 kg sphere dropped from heights h_1 = 1 m and h_2 = 5m, see Figure 2. The metallic inner structure of the beam is made by longitudinal bars, having diameter equal to 30 mm and spatial offset of 0.175 m, and by secondary transversal and longitudinal bars 0.2 m spaced and with

Figure 2: Experimental scenario at Montagnole test site

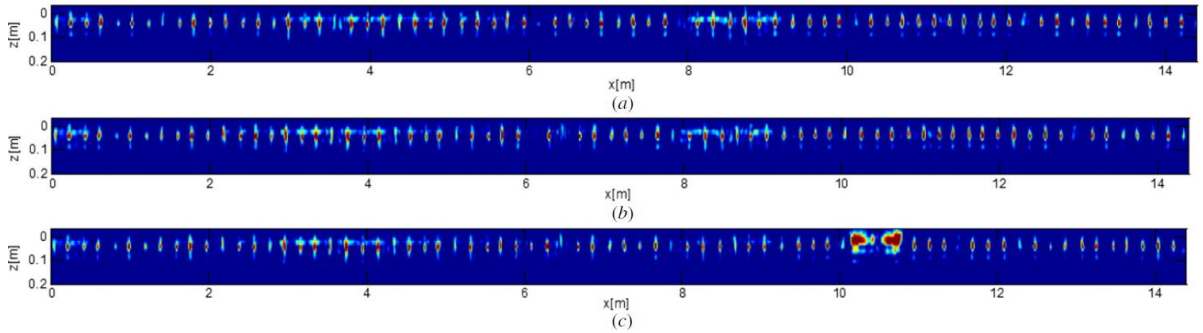

Figure 3: Tomographic images: (a) before any impact; (b) after two impacts of a steel sphere of 2500 kg falling from a height of 1 m; (c) after the impact of the sphere falling from a height of 5 m.

diameter of 10 mm.

Figures 3.a-c depict the tomographic images obtained by processing data measured before any impact, after two direct impacts from a 1 m height and after the last direct impact from a 5 m height. These three data sets have been gathered along a single B-scan aligned with the horizontal size of the beam by using a GSSI SIR 3000 system equipped with a shielded antenna, whose nominal central frequency is 1.5 GHz. The provided images clearly assess the advantages offered by MWT

enhanced GPR. As a matter of fact, not only we are able to estimate accurately the geometrical features of the reinforcement structure but also they provide an indication of the beam mechanical resistance against impacts. Specially, one can infer that the beam does not suffer significant variations except for that occurring around x = 10.5 m, that is due to the collapsed concrete at the impact point.

3 HOLOGRAPHIC RADAR RASCAN 4/4000: WORKING PRINCIPLE

This section reviews the working principle of a holographic radar system RASCAN-4/4000d esigned at the Remote Sensing Laboratory at the Bauman Moscow Technical University [7] and available at the IREA –CNR (see Figure 4). The nominal parameters of this radar system are summarized in Table 1.

Figure 4: Holographic radar system Rascan 4/4000.

Table 1: Nominal parameter of Rascan 4/4000.

Frequency range (GHz)	3.6 - 4
No. frequencies	5
Emitted power (W)	0.006
No. polarizations	2
Resolution at low depths (cm)	2
Max. penetration depth (cm)	20
Frequency range (GHz)	3.6 - 4
No. frequencies	5
Emitted power (W)	0.006
No. polarizations	2
Resolution at low depths (cm)	2
Max. penetration depth (cm)	20

Such a system is made by a probe equipped with a metric wheel and a control unit that is connected to a laptop via USB port. The probe contains three antennas, one transmitting and two receiving that simultaneously collect the backscattered field in both parallel and orthogonal polarization. The radar exploits 5 non-modulated CW signals in the frequency range [3.6-4] GHz and records, at each probe position, the amplitude of the interference pattern between the backscattered field and a reference field, i.e. the direct coupling between transmitting and receiving antennas through the investigated medium. The recorded hologram is shown on the computer's monitor in real-time.

The signal as measured at each angular frequency ω and measurement point $\mathbf{r}_m$ is given by:

$$y(\mathbf{r}_m) = A_s(\mathbf{r}_m)\exp\{j[(\omega t + \varphi_s(\mathbf{r}_m))]\} \tag{4}$$

In eq.(4), A_s denotes the signal amplitude and $\varphi_s = -2\beta R + \Delta\varphi$ its phase, β being the propagation constant in the surveyed medium, R the distance from the measurement point to the target location,

and $\Delta\varphi$ an additional phase shift introduced by the object scattering. The backscattered signal $y(\mathbf{r}_m)$ is combined with a reference signal $y_0(\mathbf{r}_m) = A_0 \exp\{j(\omega t + \varphi_0)\}$, being φ_0 a constant phase term. Hence, by getting the square amplitude of the interference signal, assuming $|A_s(\mathbf{r}_m)| \ll |A_0|$ and filtering out $|A_o|^2$ the interference signal is given as:

$$I(\mathbf{r}_m) = 2|A_s(\mathbf{r}_m)||A_0|\cos(\varphi_s(\mathbf{r}_m) - \varphi_0) \tag{5}$$

According to eq.(5), a constructive interference $\varphi_s(\mathbf{r}_m) - \varphi_0 = k\pi$ or a destructive one $\varphi_s(\mathbf{r}_m) - \varphi_0 = \pi/2 + k\pi$ may occur depending on the target distance and the working frequency. In the first case, the useful signal attains its maximum whereas in the latter case is zero so that no scattered signal is detected. In order to avoid blind depths, the radar system collects the signal at 5 different frequencies and by accounting for both parallel and orthogonal polarizations. Therefore, 10 different holograms are recorded. These are high resolution images of the constant depth sections of the geometrical features of the targets and are obtained in real time and in a simple way, i.e. without sophisticated data processing. On the other hand, RASCAN-4/4000 cannot provide any information on object's depth and shallower anomalies may create interferences, which hide the signal due to deeper objects.

As compared to GPR, the holographic radar allows to obtain a better resolution and allows to detect and achieve clear images of dielectric targets located above metallic surfaces.

4 ON THE PERFORMANCE OF RASCAN 4/4000

To point out the RASCAN's potentiality in the frame of structural monitoring, we report on two examples referred to data collected in controlled conditions at the IREA laboratory. Further example assessing the achievable performance in on filed conditions are given in [8,12].

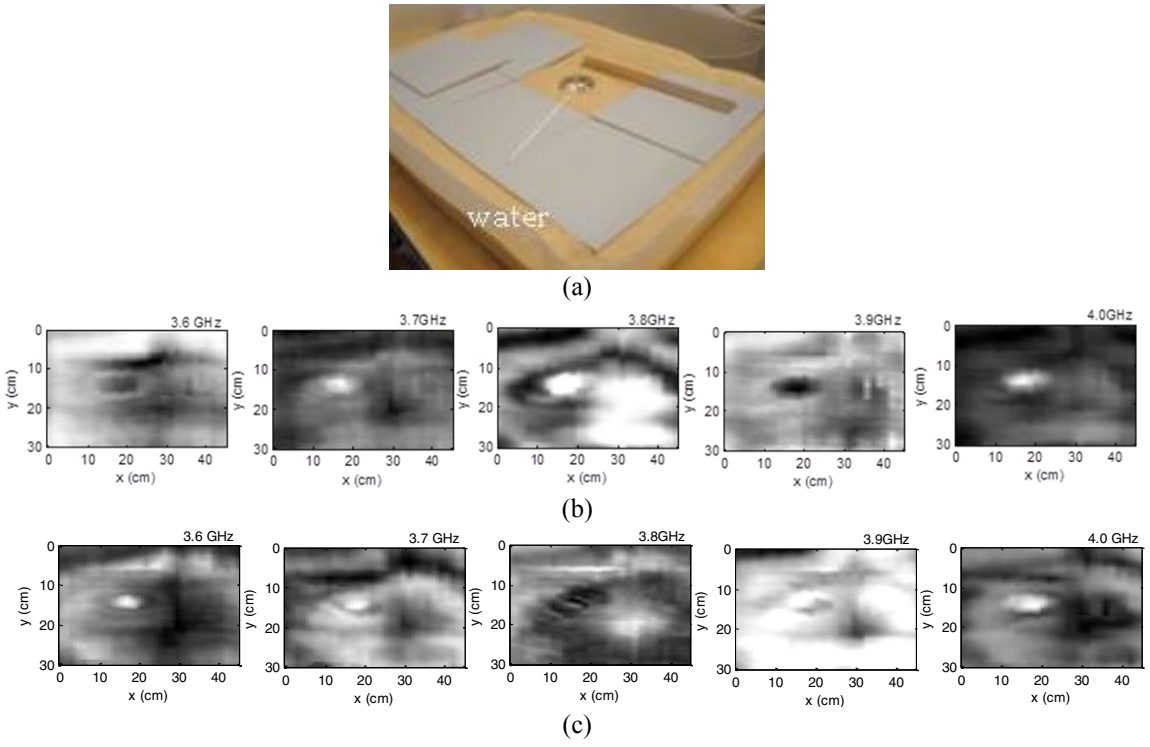

Figure 5: Imaging of a water infiltration: a) picture of the laboratory test case; b) holograms obtained by using the parallel polarization; c) holograms obtained by using the perpendicular polarization.

The first example deals with an experiment devoted to reproduce the case of a water infiltration under a tiled floor. In particular, a circular water container (radius = 4.5 cm) filled with fresh water has been placed in a sand box and covered by square ceramic tiles, whose side is 15 cm long. Holograms have been recorded by moving the radar along 30 lines, 45 cm long and spaced of 1 cm. Hence, a rectangular area whose size is 45 cm x 30 cm has been inspected. The acquisition step along each line has been fixed equal to 0.5cm.

The reference scenario and the holograms corresponding to the parallel and perpendicular polarizations are shown in Figures 5a-c. The water is more or less visible in the center-left side of all the images. These latter are the raw output of the measurement stage and corroborate the Rascan 4/4000 ability to provide high resolution holograms, which allow a reliable and fast estimation of the location and planar size of hidden anomalies.

The second example concerns the detection of a plasterboard wall. Owing to its characteristics to be economic, thin, simple to be installed, fire resistant and suitable for cutting down speech and sound transmission, plasterboard is often used to make interior walls and ceilings. Plasterboard panels are made of gypsum plaster pressed between two thick sheets of paper and are joined together with metallic junctions. Therefore, aim of the experiment was to investigate the homogeneity of a painted plasterboard wall (see Figure 6a) and localize the metallic junctions occurring among the panels. In this case, a rectangular flat domain, whose size is 120cmx40cm, was scanned by considering 20 lines spaced of 2cm. Along each line, the data was gathered with a spatial step of 0.05cm. The overall survey time was about of 10 minutes.

The holograms acquired at the parallel and perpendicular polarization are shown in Figures 6 b, c, respectively, and allow to see clearly the presence of two metallic junctures, which are about 5 cm large and far 60 cm one to the other one. From these figures one can infer that the wall has been built by using plasterboard panels of 60 cm having a layered structure along the x-axis.

(a)

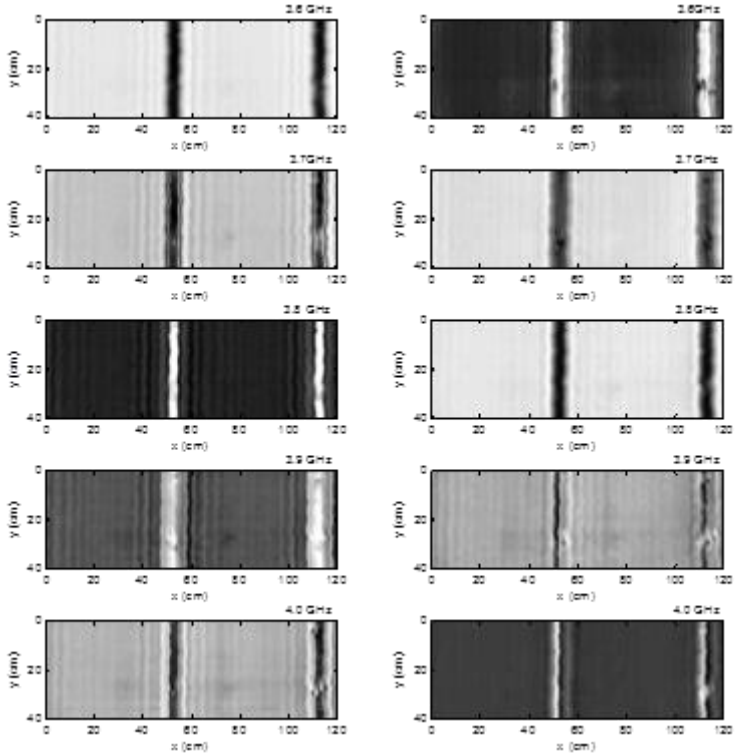

(b) (c)

Figure 6: Imaging of a water infiltration: a) picture of the laboratory test case; b) holograms obtained by using the parallel polarization; c) holograms obtained by using the perpendicular polarization.

This test case provides a proof of the RASCAN ability to monitor to quickly inspect the shallower areas of civil structures and provide information on the internal structure of a wall, like the presence of reinforcement structure or non-homogeneous elements.

CONCLUSION

The working principles and the reconstruction capabilities of two kinds of subsurface radar systems have been summarized briefly. The first one is that of MWT enhanced GPR, which is suitable for quick and good resolution surveys of the shallower layers of manmade structures. The second considered class is that of holographic radar systems. In particular, the radar Rascan-4/4000 has been presented owing to its capability of providing clear holograms of the inner features of the surveyed medium.
In order to schedule reliable and efficient diagnostic surveys devoted to state the healthy state of a structure, future activities will be addressed on the combined use of the two considered types of subsurface radar systems. The specific pursued goal will be to perform multi-resolution surveys allowing, first of all, the real-time detection of hidden anomalies, with a low rate of missing the targets, and then to provide high resolution images, from which estimate the geometrical features even in depth and possibly infer the electromagnetic parameters of the detected objects.

REFERENCES

[1] G Leone and F Soldovieri. Analysis of the distorted Born approximation for subsurface reconstruction: truncation and uncertainties effect. *IEEE Trans. Geosci. Remote Sens*., vol.41, pp.66–74, Jan. 2003
[2] G. Leucci, R. Persico and F. Soldovieri. Detection of fractures from GPR data: the case history of the Cathedral of Otranto. *J. Geophys. Eng.*, vol.4, pp.452–461, Dec. 2007.
[3] J. Hugenschmidt, A. Kalogeropoulos, F. Soldovieri. and G. Prisco. Processing strategies for high-resolution GPR concrete inspections. *NDT and E Int*., vol.3, pp. 334–42, June 2010.
[4] R. Persico, F. Soldovieri, E. Utsi. Microwave tomography for processing of GPR data at Ballachulish, *J. Geophys. Eng.,* vol.7, pp. 164-173, June 2010.
[5] I. Catapano, L. Crocco, R. Di Napoli, F. Soldovieri, A. Brancaccio, F. Pesando and A. Aiello. Microwave tomography enhanced GPR surveys in Centaur's Domus, Regio VI of Pompeii, Italy. *J. Geophys. Eng.*, vol.9, pp. S92–99. Aug.2012.
[6] I. Catapano, R. Di Napoli, F. Soldovieri, M. Bavusi, A. Loperte and J. Dumoulin. Structural monitoring via microwave tomography-enhanced GPR: the Montagnole test site. J. Geophys. Eng., vol.9, S100–S107. Aug. 2012.
[7] S. Ivashov, I.A. Vasiliev, T.D. Bechtel, and C. Snapp. Comparison between impulse and holographic subsurface radar for NDT of space vehicle structural materials. *Prog. Electromagn. Res*., vol.3, pp.658–661, 2004.
[8] E. Bechtel, S. Ivashov, T. Betchel, E. Arsenyeva, A. Zhuravlev, I. Vasiliev, V. Razevig, and A. Sheyko. Experimental determination of the resolution of the RASCAN-4/4000 holographic subsurface radar system. *12th International Conference in Ground Penetrating Radar Proceedings*, Birmingham, UK, 16–19 June, 2008.
[9] D. J. Daniels. *Ground Penetrating Radar*. IEE Radar, Sonar and Navigation Series vol.15, London, UK: IEE 2004.
[10] M. Bertero and P. Boccacci. *Introduction to Inverse Problems in Imaging*. Bristol, UK: Institute of Physics Publishing, 1998.
[11] M. Proto et al., Transport Infrastructure surveillance and monitoring by electromagnetic sensing: the ISTIMES project. Sensors, vol.10, pp.10620–10639, 2010.
[12] I. Catapano, L. Crocco, A. F. Morabito, F. Soldovieri. Tomographic imaging of holographic GPR data for non-invasivestructural assessment: the Musmeci bridge investigation. *NDT and E Int*, 2012.